

Short Communication

Preparation of Carbon Nanotube/MnO₂ Nanocomposite as an Electrode Modifier for Prostate-Specific Antigen (PSA) Determination

Zhengang Gu, Ming Zhao, Wencai Zhang, Tao Jiang and Maoli Sun *

Department of Urology, The Third Affiliated Hospital of Qiqihar Medical University, Qiqihar; Heilongjiang Province, 161000, P.R. China

*E-mail: sunmaoli741@163.com

Received: 20 June 2017 / Accepted: 18 August 2017 / Published: 12 October 2017

In this study, prostate-specific antigen (PSA) was determined based on a selective and sensitive electrochemical sensor by utilizing nanotechnology and a surface imprinting strategy. Manganese nanoparticle-decorated multiwalled carbon nanotubes (MWCNTs) were used as a nano-iniferter for the construction of a three-dimensional molecularly imprinted polymer matrix for PSA detection using controlled radical polymerization. The differential pulse stripping voltammetric and square wave techniques were used to confirm the excellent analytical behaviour of our sensor towards PSA determination.

Keywords: Prostate specific antigen; Imprinting and nanotechnology; Multiwalled carbon nanotubes; Electrochemical determination; Manganese nanoparticles

1. INTRODUCTION

Prostate-specific antigen (PSA) is a serine protease that has a physiological function in seminal fluid liquefaction. In the case of prostate cancer, PSA is released into the circulatory system, leading to a 10⁵-fold increase in the concentration level in blood. Benign prostate diseases can also lead to an increase in PSA levels. From diagnosis to response monitoring for treatment, PSA testing has gained widespread application as a cancer marker to help predict the risk of prostate cancer, as well as provide better treatment. The more extensive use of PSA screening has led to a divergence of views for its efficacy. Some hold that PSA screening is responsible for the diagnosis and treatment of prostate cancers that do not actually pose a threat and, therefore, more importantly, does not reduce prostate cancer mortality. The critical PSA level required to warrant biopsy has been controversial. PSA testing

can be viewed as a risk indicator rather than an all-encompassing technique that can resolve all prostate cancer related problems. In this study, the relationship between PSA and the risk, disease outcome and recurrence of prostate cancer was investigated. The application of PSA testing for the prediction of prostate cancer over the long term was also studied, together with the application of PSA derivatives such as PSA dynamics and PSA subforms for PSA test improvement. The PSA transcription is controlled by androgens, leading to a restriction on the high-level production in the prostate epithelium. The synthesis of PSA occurs in healthy prostate tissue, in benign prostatic hypertrophy (BPH) and in prostate cancer of all grades and stages [1, 2]. PSA is released in seminal fluid, in which the PSA concentration range is 0.3 - 3 mg/ml (10–100 μ M/L) [3]. Most of the PSA is an active serine protease having chymotrypsin-like activity, usually contributing to the proteolysis of gel proteins of seminal fluid [4]. Hence, PSA possesses the physiological function of seminal fluid liquefaction [5].

Following approval by the US Food and Drug Administration, PSA was used as a marker for the monitoring of patients treated for prostate cancer in 1986, as well as a diagnostic marker in 1994. The extensive use of PSA-based screening in the US has caused an increase in the diagnosis of prostate cancer as well as stage migration, with a decreased proportion of metastatic or locally advanced cancers at diagnosis [6-9]. Different levels of circulating PSA in blood can lead to varying risks for prostate cancer [10-14]. Nevertheless, there are some difficulties in evaluating the value of PSA screening. The comparisons made between different reports can be inaccurate because PSA levels in serum are different according to different age and other factors, for example. Furthermore, the majority of the reports on PSA testing are vulnerable to verification bias, as shown in the latter part of this work.

An increase in the PSA level typically suggests that a prostate biopsy is warranted, with a conventional critical value for the PSA concentration of 4 ng/ml. For those diagnosed with the above critical value, the cancer detection rate ranges from 27 to 44%, based on three reports using large cohorts subject to extensive prior screening [15-18]. Since biopsy leads to little detection of the prostate cancer status of men with low PSA levels, it is tougher to confirm the sensitivity and specificity of PSA testing. Fortunately, the Prostate Cancer Prevention Trial (PCPT) is unique in that all participants are required to receive biopsy treatment. Among the 5,112 men in the placebo arm of the above experiment, the sensitivity and specificity for the case of a PSA level above 4 ng/ml were 24% and 93%, respectively [19].

The critical value of approximately 4 ng/ml has been the subject of controversy; it is either too strict or too lenient. It has been proposed through extensive literature that those men with a PSA level lower than 4 ng/ml and diagnosed with prostate cancer are not rare. For instance, among the men with a median age of 72 years in the placebo arm of the PCPT, through biopsy, 27% of those with 3.1–4 ng/mL PSA were detected to have prostate cancer, while 6.6% of men with lower than 0.5 ng/ml PSA were detected to have prostate cancer. Similarly, in the case of a large-scale European investigation, the cumulative prostate cancer detection rate of men with 2.0–2.99 ng/ml PSA ranged from 21 to 25%, while that of men with 3.0–3.99 ng/mL PSA was 33%. Nevertheless, according to the results, particularly from the PCPT, the decreased critical value for PSA led to increased sensitivity as well as increased specificity, with the absence of a cut-off point contributing to the increase in specificity and

sensitivity. There has been a popular belief that the sole use of a PSA test with a critical value for suggesting a prostate biopsy is not appropriate. However, consensus has not been reached on this view. The first reason is that a single critical value cannot be used to divide men into two homogenous groups, with high and low cancer risk [20]. In addition, there are other factors that determine whether men choose a biopsy or not, including race, heredity, age, personal preference, and concurrent disease. Therefore, the calculation of the possibility of prostate cancer using the PSA level, as well as other cancer risk predictors, has gained increasing attention, and has been offered to patients as a reference for biopsy. To offer a successful estimate for cancer risk, instead of a binary positive or negative test result, PCPT experts have developed an online calculator using PSA and additional risk-contributing factors [21].

Besselink and others [22] reported the detection of PSA based on a surface plasmon resonance (SPR) sensor fabricated using colloidal gold and latex microspheres (diameter, 120 nm) coated onto the surface of planar- and gel-type sensors. In comparison with experiments performed in the absence of amplification, the use of colloidal gold contributed to a significant increase in detection sensitivity (of approximately three orders of magnitude). The limit of detection (LOD) was calculated to be 0.15 ng/mL, which is low enough for measurement of enhanced, clinically relevant PSA levels. Soukka and co-workers [23] reported a two-step immunoassay for the detection of free PSA based on monoclonal anti-PSA antibody coated europium(III) chelate nanoparticles. The measurement was carried out by using a low-fluorescence microtitration well passively coated by a monoclonal anti-PSA antibody. On the other hand, direct measurement of the europium(III) fluorescence from the well bottom was achieved by using a standard time-resolved microtitration plate fluorometer. Wu et al. [24] prepared a PSA sensor by the attachment of PSA antibodies onto a gold-coated silicon nitride microcantilever. A specimen containing PSA was passed over the surface of the cantilever (which has the appearance of a microscopic diving-board-shaped mechanical structure). By using a laser beam to monitor deflection in the microcantilever, binding of the PSA to the antibodies could be observed. In this way, PSA was detected in a concentration range of 0.2 ng/mL to 60 mg/mL.

In this report, a surface imprinted polymer to detect trace levels of PSA was fabricated using a nano-iniferter synthesized based on MnO₂ nanoparticle-modified MWCNTs. Our developed PSA sensor was used for the detection of PSA in blood serum specimens. Square wave and differential pulse stripping voltammetry (SWSV and DPSV), chronocoulometry (CC), cyclic voltammetry (CV), and XRD measurements were performed to characterize the PSA sensor. Our developed sensor showed simplicity, ease of operation, short determination period, and excellent selectivity and specification, and was successfully used for the determination of trace level PSA in the absence of any cross-reactivity.

2. EXPERIMENTS

2.1. Synthesis of CNT/MnO₂ composites

CNTs (multi-walled CNTs) were sourced commercially from Shenzhen Nanotech Port. Impurities such as catalyst particles were removed from the CNTs by reflux in 10 wt% nitric acid for 0.5 h for further use. All other test chemicals were of analytical reagent grade and used without

additional purification. The CNT/MnO₂ hybrids were prepared by first dispersing purified CNTs (0.1575 g) into distilled water (100 mL) using ultrasonic vibration for 6 h and then mixed with a given amount of KMnO₄ and stirred for 60 min to allow for sufficient absorption of the KMnO₄ onto the walls of the CNTs. This was followed by heating of the mixed solution in a household microwave oven. After microwaving for 10 min, the mixture was left to cool naturally down to ambient temperature. Finally, the as-prepared suspension was filtered, followed by several washing cycles using distilled water and absolute alcohol, together with drying in a vacuum oven at 100 °C for 12 h. The final product was obtained in the form of a black powder, which was decanted before use.

2.2. Characterization methods

X-ray powder diffraction (XRD, TTR-III) with Cu K α radiation was used for the determination of the crystallographic structures of the test materials. A Kratos AXIS Ultra X-ray photoelectron spectrometer equipped X-ray photoelectron spectroscopy (XPS) was used for the chemical state analysis. This study also used a monochromatic Al source at 210 W, with a pass energy and step of 20 eV and 0.1 eV, respectively. The C 1s line at 284.6 eV was used for the correction of all XPS spectra obtained. A CH instrument (USA, model number 660 C) equipped with a triple-cell configuration (the working electrode, a MIP-modified PGE electrode; the reference electrode, an Ag/AgCl (3.0 M KCl); the counter electrode, a platinum wire) was used for electrochemical characterization, including CC, CV, SWSV, and DPSV. All measurements were carried out at 25 \pm 1 °C (ambient temperature).

2.3. Fabrication of PSA sensor

Pencil rods were initially treated using nitric acid (6 M) for 15 min, followed by washing with water and rubbing with soft cotton for surface smoothing. Subsequently, the pencil rod was inserted into a micro tip, and then a metallic wire was soldered onto the opposite end of the rod for electrical contact. This was followed by drop-coating of the PGE tip using a 5 μ l suspension of the nano-iniferter (5 mg) dispersed into DMSO solution (4 mL). Polymerization on the surface of the PGE was achieved by mixing EGDMA (2 mM, 0.37 mL), 0.1 mL of CNT/MnO₂ and 6 mg of PSA (dissolved in 0.2 mL of DMSO) with 0.2 mmol of itaconic acid (25 mg, dissolved in 0.3 mL of DMSO) in a glass vial and then purging with N₂ for 10 min. This was followed by drop-coating of the pre-polymer solution onto the nano-iniferter-decorated PGE tip under heat treatment at 50 °C for 120 min, to yield the adduct-decorated PGE (template inside the polymer matrix). We also fabricated a non-imprinted polymer (NIP)-decorated PGE without PSA as the control group.

2.4. Electrochemical measurement

CC and CV measurements were performed to qualitatively detect the PSA, while the DPSV and SWSV techniques were used for quantitative determination in clinical and aqueous specimens.

PSA-imprinted polymer decorated PGE (PSA-sensor) was prepared by placing the adduct-decorated PGE in a NaOH solution (0.1 M) under dynamic conditions for 45 min to extract the template. The electrode was then taken out of the extraction solvent and washed repeatedly using distilled water ($n=3$, 0.5 mL) to prevent any carryover of the analyte. This was followed by PSA determination in an electrochemical cell that contained KCl solution (10.0 mL, pH 10.0). For the CV measurement, the scan rates range from 0.02 to 0.4 V/s, and the potential window ranged from +1.8 to -0.2 V. SWSV and DPSV were obtained for voltages between +1.2 and +0.4 V (pulse width, 50 ms; pulse amplitude, 25 mV); for this measurement, the potential was -0.5 V, and the accumulation time was 0.5 min.

3. RESULTS AND DISCUSSION

The characteristic XRD profiles of the CNT/MnO₂ composites are shown in Fig. 1A. The data show that carbon and birnessite-type MnO₂ (JCPDS 42-1317) are present with mixed crystalline and amorphous components. XPS was used to characterize the CNT/MnO₂ surface. As shown in Fig. 1B, the survey spectrum exhibits peaks of Mn 2p_{1/2} (centred at 653.7 eV), Mn 2p_{3/2} (centred at 642.2 eV), C 1s, and O 1s. The spin-energy separation with respect to the two Mn peaks was determined to be 11.7 eV, as indicated in Fig. 1C. This is consistent with the reported data for Mn 2p_{1/2} and Mn 2p_{3/2} in MnO₂.

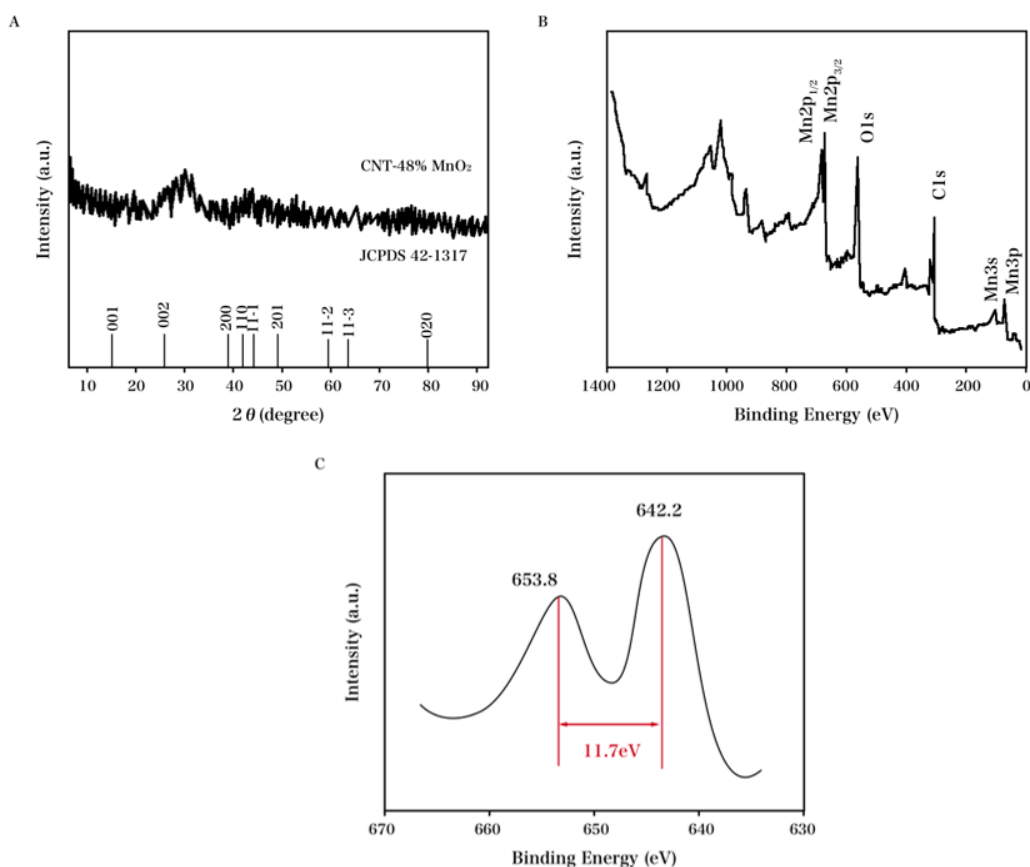


Figure 1. (A) Characteristic XRD profiles of the CNT/MnO₂ hybrids. (B) XPS patterns and (C) the magnification of Mn 2p region of the CNT/MnO₂ samples.

Fig. 2A and Fig. 2B shows the data obtained from square wave voltammetric and CV measurements, which were carried out to study the electrochemical performance of the nano-iniferter using MWCNTs and CNT/MnO₂ coated PGE; the electrochemical probe molecule was K₄Fe(CN)₆ (0.1 M). In the CVs and SWSVs, an approximately 2-fold and 4-fold increase in current was observed for the CNT/MnO₂ composite, respectively. It can be seen that the CNT itself shows a good electrical conductivity due to its conductive nature. On the other hand, the incorporation of MnO₂ into CNT can further enhance the conductivity of the electrode, which is favourable for usage in electrochemical determination [25].

For the MIP-decorated PGE, CV measurement was performed using PSA (3.99 μg/L) to obtain optimal parameters. As the scan rate is increased, a single cathodic peak recorded at +0.7 V first shifts upwards and then shifts to a more negative potential (Fig. 3). This is due to the high stability of the MIP–PSA adduct, leading to the requirement of a high energy for cathodic reduction. The peak current was found to be linearly correlated to the scan rate that ranged from 0.02 to 0.40 V/s. The surface concentration of the electroactive species (Γ) for the PSA was determined to be 7.9×10^{-8} mol/cm², as shown by the slopes in the linear plots of peak current (I_p) vs. scan rate (ν). The reduction in PSA is an adsorption-controlled process, which can be used to preconcentrate a micro-quantity of PSA onto the surface of MIP-modified PGE for quantitative analysis. The reduction reaction process was attributed to the two-electron, two-proton reduction of the di-sulfide bond present in the protein molecule to free thiol groups [26, 27].

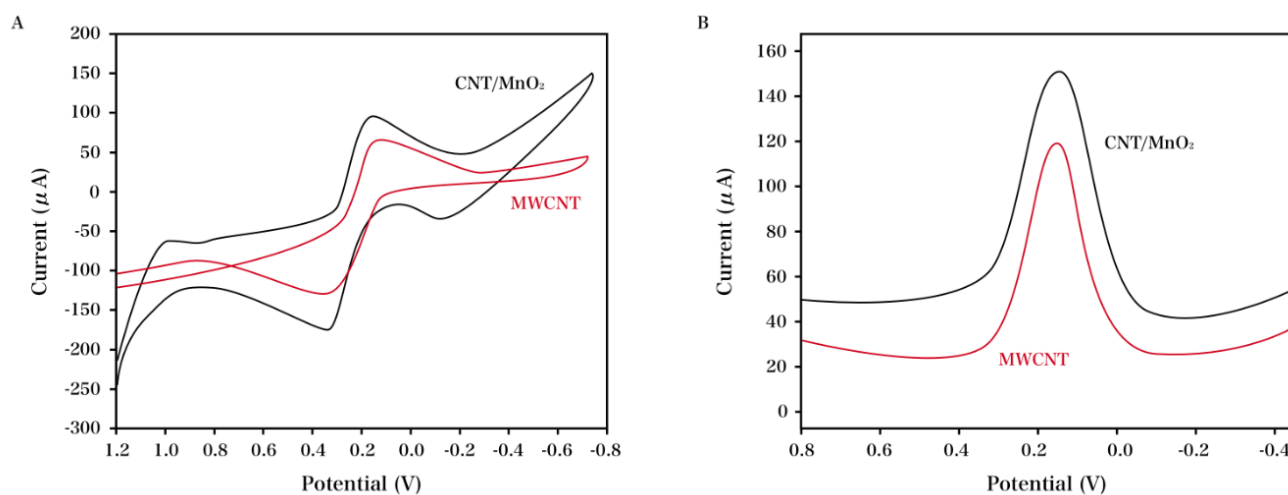


Figure 2. (A) CV profiles and (B) SWSV profiles of MWCNTs and CNT/MnO₂ coated PGE in K₄Fe(CN)₆ (0.1 M)

SWSV and DPSV measurements were performed for PSA of varying concentrations using the same operating parameters for the sensor as determined for PSA in optimized conditions. A linear relationship was observed between the DPSV current increase and the PSA concentration (Fig. 4A and Fig. 4B). The DPSV current response towards PSA in the lower and higher concentration ranges is shown in Fig. 4A and Fig. 4B, respectively.

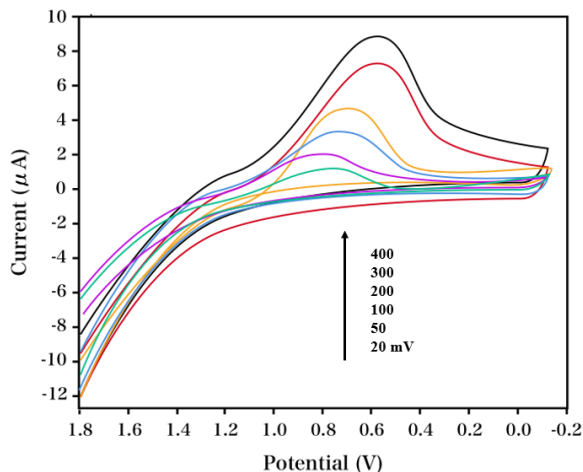


Figure 3. CV profiles of 3.99 $\mu\text{g/L}$ PSA recorded for a scan rate ranging from 0.02 to 0.4 V/s.

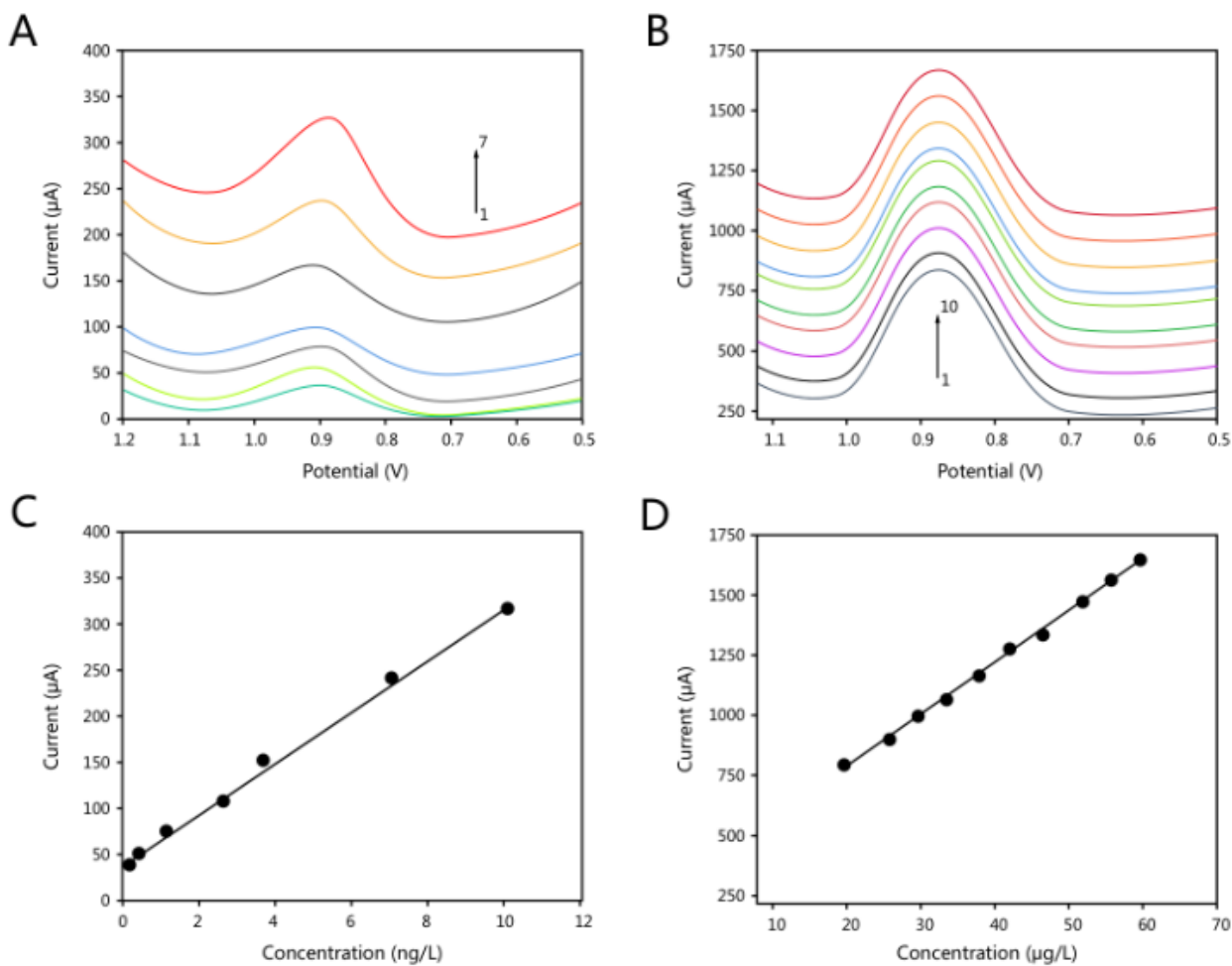


Figure 4. DPSV response obtained at the MIP-decorated PGE in the presence of PSA with varying concentrations: (A) lower detection range (0.01–10 ng/L) and (B) higher detection range (20–62 $\mu\text{g/L}$).

Notably, two linear ranges are observed with a transition point at 10.0 ng/L, as shown in the PSA concentration *vs.* current profile. Analysis of the DPSV data reveals that the two linear ranges of our developed sensor occur at 10 pg/L to 10 ng/L and 20 ng/L to 62 $\mu\text{g/L}$, respectively. The LOD of our developed sensor was calculated to be 3.04 pg/L based on the definition from the International Union of Pure and Applied Chemistry (IUPAC). The low detection limit can be attributed to the complementarity of the size, shape and position of recognition functional groups between PSA and the binding sites present in the MIP matrix.

Fig. 5A and Fig. 5B show data obtained from SWSV measurements, which were also used for the quantitative determination of the sensor performance in the high and low PSA concentration range and the sensitivity of our sensor towards PSA. Fig. 5A shows the SWSV current response towards PSA in the lower concentration range, while Fig. 5B showed that in the higher concentration range. It can be seen that the strategy we have developed has the potential for application to the detection of human body PSA under both normal and abnormal conditions. The analytical features of our developed biosensor are compared with those found in previous studies in Table 1.

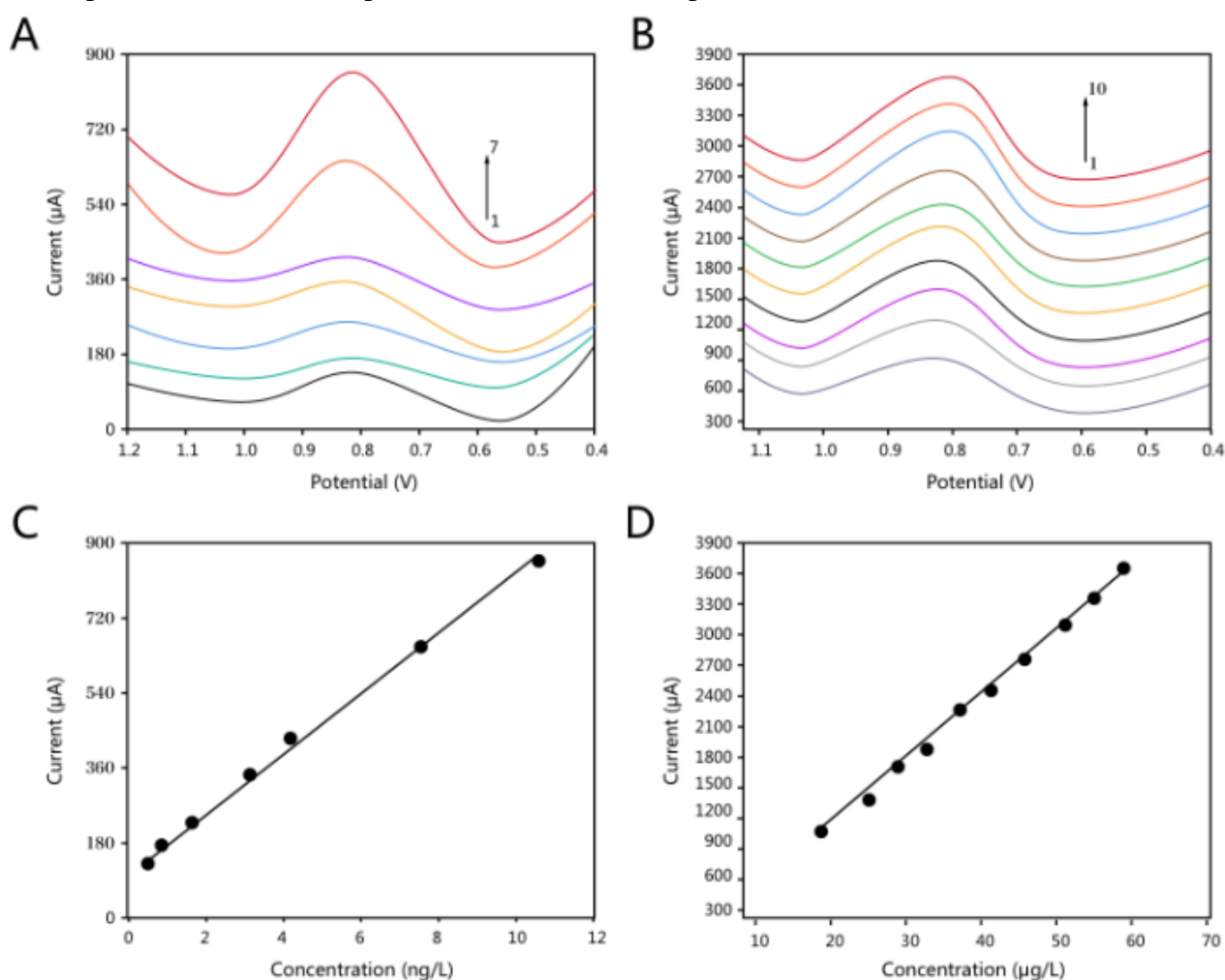


Figure 5. SWSV response obtained at the MIP-decorated PGE in the presence of PSA (varying concentration): (A) 0.01–10 ng/L and (B) 20–62 $\mu\text{g/L}$; the pH value, accumulation potential, and accumulation time were optimized as 10, -0.5 V, and 0.5 min, respectively.

Table 1. Comparison of the major characteristics of electrochemical sensors used for the detection of PSA.

Electrode	Linear detection range	Detection limit	Reference
QDots based immunosensor	0.5-80 ng/mL	0.2 ng/mL	[28]
NP labelled-IEB	0.05–4 ng/mL	20 pg/L	[29]
SWNTs labeled immunosensor	1-100 ng/L	0.25 ng/mL	[30]
MIP-decorated PGE	0.01–10 ng/L and 20–62 μ g/L	3.04 pg/L	This work

To investigate the selectivity of our PSA-sensor, the SWSV response towards PSA at MIP- and NIP-decorated PGEs was compared with that of interference agents such as citric acid (CA), tyrosine (Tyr), arginine (Arg), glutamic acid (GA), histidine (His), lysine (Lys), albumin (Alb), globulin (Glo), uric acid (UA), ferritin (fer), urea, insulin (Ins), NaCl, and a mixture of these agents (Mix). Both MIP and NIP-decorated PGEs showed a current response towards all the above substances including PSA and interference agents. However, following a washing treatment with water, the response of all the test substances, except for PSA, was determined to be negligible, confirming that some non-specific binding of the analyte molecules, which can be easily eliminated upon washing with water, was the contributing factor to the current recorded on the MIP-decorated PGE. In addition, the MIP-decorated PGE exhibited a 100% current response for the target PSA molecule in the presence of a mixture of PSA and other interfering agents. Compared with PSA, citric acid and tyrosine exhibited similar peak potential and identical current height as that determined for the unmodified PGE. We also determined the PSA level in urine and serum samples. As shown in Table 2, the fabricated electrochemical sensor demonstrated outstanding accuracy for PSA detection.

Table 2. Recoveries of as-proposed sensor for the detection of PSA in urine and serum.

Sample	Added (μ g/mL)	Found (μ g/mL)	Recovery (%)	RSD (%)
Urine 1	30	29.78	99.27	3.64
Urine 2	50	50.22	100.44	1.42
Serum 1	30	28.97	96.57	2.65
Serum 2	50	48.66	97.32	4.33

4. CONCLUSIONS

In this work, an imprinted sensor was fabricated and successfully used for excellent electrochemical determination of protein cancer biomarkers in men and women sera, with the realization of desirable accuracy, reproducibility and sensitivity. A PSA-imprinted polymeric film was formed onto a surface covered with Mn nanoparticle-modified MWCNTs, which enabled controlled radical polymerization and the implementation of a surface imprinting strategy. The proposed PSA

electrochemical sensor demonstrates two linear detection ranges: 0.01–10 ng/L and 20–62 µg/L, with a low LOD of 3.04 pg/L.

References

1. A.M. Herrala, K.S. Porvari, A.P. Kyllönen and P.T. Vihko, *Cancer*, 92 (2001) 2975.
2. S. Lintula, J. Stenman, A. Bjartell, S. Nordling and U.H. Stenman, *The Prostate*, 63 (2005) 324.
3. G. AHLGREN, G. RANNEVIK and H. LILJA, *Journal of andrology*, 16 (1995) 491.
4. H. Lilja, J. Oldbring, G. Rannevik and C. Laurell, *Journal of Clinical Investigation*, 80 (1987) 281.
5. H. Lilja, *Journal of Clinical Investigation*, 76 (1985) 1899.
6. J.O. Ung, J.P. Richie, M.-H. Chen, A.A. Renshaw and A.V. D'Amico, *Urology*, 60 (2002) 458.
7. R. Gao, Z. Cheng and J. Choo, *Lab on a Chip*, 16 (2016) 1022.
8. Q.-M. Feng, J.-B. Pan, H.-R. Zhang, J.-J. Xu and H.-Y. Chen, *Chemical Communications*, 50 (2014) 10949.
9. I. Strzemińska, S.S.R. Fanchine, G. Anquetin, S. Reisberg, V. Noël, M. Pham and B. Piro, *Biosensors and Bioelectronics*, 81 (2016) 131.
10. G. Aus, J.-E. Damber, A. Khatami, H. Lilja, J. Stranne and J. Hugosson, *Archives of internal medicine*, 165 (2005) 1857.
11. P.H. Gann, C.H. Hennekens and M.J. Stampfer, *Jama*, 273 (1995) 289.
12. U.-H. Stenman, J. Leinonen, M. Hakama, P. Knekt, A. Aromaa and L. Teppo, *The Lancet*, 344 (1994) 1594.
13. I.M. Thompson, D.K. Pauler, P.J. Goodman, C.M. Tangen, M.S. Lucia, H.L. Parnes, L.M. Minasian, L.G. Ford, S.M. Lippman and E.D. Crawford, *N. Engl. J. Med.*, 350 (2004) 2239.
14. D. Ulmert, A.M. Serio, M.F. O'Brien, C. Becker, J.A. Eastham, P.T. Scardino, T. Bjork, G.r. Berglund, A.J. Vickers and H. Lilja, *Journal of Clinical Oncology*, 26 (2008) 835.
15. G.L. Andriole, D.L. Levin, E.D. Crawford, E.P. Gelmann, P.F. Pinsky, D. Chia, B.S. Kramer, D. Reding, T.R. Church and R.L. Grubb, *Journal of the National Cancer Institute*, 97 (2005) 433.
16. E.D. Crawford, E.P. DeAntoni, R. Etzioni, V.C. Schaefer, R.M. Olson, C.A. Ross and T.P.C.E. Council, *Urology*, 47 (1996) 863.
17. J. Hugosson, G. Aus, H. Lilja, P. Lodding and C.G. Pihl, *Cancer*, 100 (2004) 1397.
18. W. Deng, C. Chu, S. Ge, J. Yu, M. Yan and X. Song, *Microchimica Acta*, 182 (2015) 1009.
19. I.M. Thompson, C. Chi, D.P. Ankerst, P.J. Goodman, C.M. Tangen, S.M. Lippman, M.S. Lucia, H.L. Parnes and C.A. Coltman, *Journal of the National Cancer Institute*, 98 (2006) 1128.
20. I.M. Thompson, D.P. Ankerst, C. Chi, M.S. Lucia, P.J. Goodman, J.J. Crowley, H.L. Parnes and C.A. Coltman, *Jama*, 294 (2005) 66.
21. I.M. Thompson, D.P. Ankerst, C. Chi, P.J. Goodman, C.M. Tangen, M.S. Lucia, Z. Feng, H.L. Parnes and C.A. Coltman, *Journal of the National Cancer Institute*, 98 (2006) 529.
22. G.A. Besselink, R.P. Kooyman, P.J. van Os, G.H. Engbers and R.B. Schasfoort, *Analytical biochemistry*, 333 (2004) 165.
23. T. Soukka, J. Paukkunen, H. Härmä, S. Lönnberg, H. Lindroos and T. Lövgren, *Clinical chemistry*, 47 (2001) 1269.
24. G. Wu, R.H. Datar, K.M. Hansen, T. Thundat, R.J. Cote and A. Majumdar, *Nature biotechnology*, 19 (2001) 856.
25. B. Rezaei, O. Rahmanian and A.A. Ensafi, *Sensors and Actuators B: Chemical*, 196 (2014) 539.
26. J.H. Choi, H.S. Kim, J.-W. Choi, J.W. Hong, Y.-K. Kim and B.-K. Oh, *Biosensors and Bioelectronics*, 49 (2013) 415.
27. G.A. Suaifan, C. Esseghaier, A. Ng and M. Zourob, *Analyst*, 138 (2013) 3735.
28. J. Wang, G. Liu, H. Wu and Y. Lin, *Small*, 4 (2008) 82.
29. Y.-Y. Lin, J. Wang, G. Liu, H. Wu, C.M. Wai and Y. Lin, *Biosensors and Bioelectronics*, 23 (2008)

1659.

30. J. Okuno, K. Maehashi, K. Kerman, Y. Takamura, K. Matsumoto and E. Tamiya, *Biosensors and Bioelectronics*, 22 (2007) 2377.

© 2017 The Authors. Published by ESG (www.electrochemsci.org). This article is an open access article distributed under the terms and conditions of the Creative Commons Attribution license (<http://creativecommons.org/licenses/by/4.0/>).